NO_x Estimation in Diesel Engines via In-Cylinder Pressure Measurement

Simone Formentin, Matteo Corno, Harald Waschl, Daniel Alberer, and Sergio M. Savaresi

I. Introduction and Motivation

MAINLY due to their high fuel efficiency, diesel engines are widely used for both on-road and off-road heavy duty (HD) applications. As it is well known, besides the desired mechanical power output, combustion produces undesired gaseous emissions. While hydrocarbons and carbon monoxides are caused by incomplete combustion, nitrogen oxides (NO_x) are always present during standard Diesel combustion (see [1]) and therefore suitable control strategies employing emission measurements are required.

On the one hand, cost-efficient NO_x sensors, e.g., electronic metal oxide devices, are available but characterized by limitations in operating range at high temperatures, signal drift, low sensitivity, and high power consumption. On the other hand, high sensitivity devices, e.g., NO_x optical sensors, are expensive and need sophisticated support equipments (for further details, see [2]). The use of a virtual sensor may represent an interesting alternative.

To design NO_x estimators, proper models are required. However, modeling emissions is not straightforward and there is substantial potential for improvement. The existing approaches range from detailed 3-D computational fluid dynamics (CFD) models with chemical reaction kinetics [3], phenomenological models [4], zero-dimensional, and multizone models [5], [6] to purely empirical models [7]. CFD models have the potential of being very accurate, but the large number of degrees of freedom leads to poorly conditioned problems. Empirical models can be very efficient, but their accuracy depends on the choices of the regressors, i.e., the measurable variables used to estimate the NO_x value. The ideal objective in the latter case would be to estimate NO_x using as few regressors as possible.

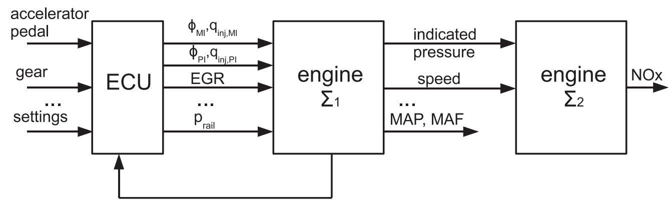

Fig. 1. Block diagram for NO_x generation. Airpath and combustion intermediate quantities are generated by (ECU controlled) engine subsystem Σ_1, whereas NO_x emissions are the output of engine subsystem Σ_2, fed by the information of indicated pressure. Only a few variables are reported: ϕ_{MI} and ϕ_{PI} are the angles of main and pilot injection, $q_{\text{inj},MI}$ and $q_{\text{inj},PI}$ refer to the quantity of main and pilot injection, EGR is the position of the exhaust gas recirculation valve, p_{rail} is the value of the rail pressure, MAF and MAP indicate the mass air flow and the manifold absolute pressure, respectively.

In the context of empirical model-based estimation, both combustion and airpath variables are employed (see [8]), thus leading to complex model structures with the need of modeling a complex chain of agents (that from now on will be conceived as in Fig. 1). In [9], only statistical pressure-based parameters are considered, and it is shown that, using 13 of them, it is possible to accurately reconstruct the NO_x trajectory during standard cycles. Unfortunately, a very large dataset is needed and the computational load is heavy. Moreover, the pressure features are not representative of the whole pressure sequence, as they are not sufficient to reconstruct the profiles.

This brief focuses on indicated pressure measurement[1] based estimation of NO_x emissions of an off-road HD Diesel engine. The goal is to develop an efficient method that uses the pressure information. Since the method avoids thermodynamical process calculation, it is be suitable for online applications. The initial motivation for this brief is based on the standing assumption that all combustion phenomena—including the NO_x formation—are reflected by the crank angle resolved pressure trajectory.

The proposed method is organized in two steps. First, a principal component analysis (PCA) is employed to extract useful information from the pressure trajectory in order to

[1]Measurement of the pressure in the combustion chamber during the combustion event.

Manuscript received September 5, 2012; revised March 1, 2013; accepted March 5, 2013. Manuscript received in final form March 6, 2013. Date of publication March 29, 2013; date of current version December 17, 2013. This work was supported in part by COMET Program is funded by the Austrian Federal Government and the Federal State Upper Austria and the Scientific Partners of ACCM. Recommended by Associate Editor K. Butts.

S. Formentin, M. Corno, and S. M. Savaresi are with the Dipartimento di Elettronica, Informazione e Bioingegneria, Politecnico di Milano, Milano 20133, Italy (e-mail: simone.formentin@gmail.com; corno@elet.polimi.it; savaresi@elet.polimi.it).

H. Waschl and D. Alberer are with the Institute for Design and Control of Mechatronical Systems, Johannes Kepler University Linz, Linz A-4040, Austria (e-mail: harald.waschl@jku.at; daniel.alberer@jku.at).

Color versions of one or more of the figures in this paper are available online.

provide a low dimensional set of input candidates for NO_x modeling. In detail, it will be shown that only four "indirect" variables are sufficient to reconstruct the pressure profiles.

In the second step, a simple static NO_x emission model is developed based on the reduced set of inputs and the application of L_2 regularization. Since NO_x emissions are expressed in the time domain, while the pressure measurements are crank angle based, the engine speed, always available on-board, is employed to provide a link between crank angle domain and time domain (this fact also explains why the NO_x generation mechanism has been illustrated as in Fig. 1). It will be shown that the physically motivated consideration of engine speed as an additional input for the NO_x model provides a satisfactory estimation accuracy for the whole engine operating range.

The proposed algorithm has a very low computational cost. This feature makes the approach appealing from a practical point of view, as it makes it suitable for the implementation of the NO_x estimator in real-world Electronic Control Unit (ECU).

The remainder of this brief is as follows. In Section II, a PCA approach for extracting pressure information using a limited set of variables is proposed. Such quantities are considered as candidate inputs for an emission model in Section III, where estimation and regularization techniques are employed to design a reliable model for NO_x estimation. The results of the above methods on a HD engine are shown in Section IV, where the validation on two different standard test cycles is provided. The note is ended by some concluding remarks. Throughout this brief, the values of pressure and NO_x (in terms of mass) will be suitably scaled and normalized for confidentiality reasons.

II. In-Cylinder Pressure Feature Extraction

As already stated, in-cylinder pressure is physically related to NO_x emissions and thus is suitable as input of an estimation model. In-cylinder pressure transducers provide crank angle-based measurements, and for each cycle typically hundreds of points are used to describe the indicated profile. As a matter of fact, provided the resolution of the crank angle measure is 1°, each cycle of a four stroke engine has 720 crank angle degrees, but only 360 are significant for emissions, whereas the others are representative for the gas exchange. Since 360 inputs would make the model useless in practice (the variance of the estimation strongly depends on the number of inputs, see [10]), in the literature some derived variables have been employed and variable selection is done by reasoning on the physics of emission production (see [9]). Two commonly used inputs are the location of 50% of fuel mass fraction burned (MFB50) and the maximum heat release. The MFB50 parameter is strongly correlated to the production of nitrogen oxides and the maximum heat release and its location may provide a measure of initial oxidation rates and reflect NO_x production. Other inputs are geometrically derived from the pressure profile, like the maximum pressure and the angle related to it, the maximum gradient of the pressure and the mean effective pressure.

These quantities are not sufficient to reconstruct the pressure profile, since the relationship used to derive them is not

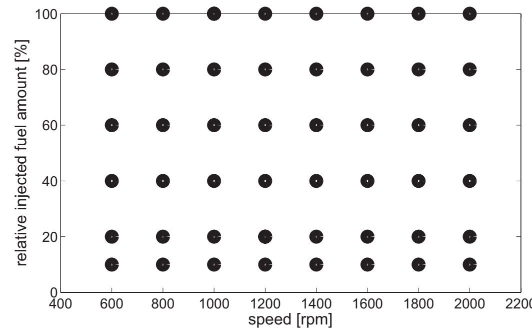

Fig. 2. Engine map and considered operating points. In the figure, 100% injected fuel amount corresponds to maximum torque at the corresponding engine speed.

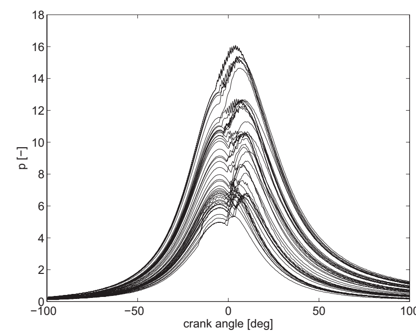

Fig. 3. Spread of in-cylinder pressure profiles for 48 engine operating points along 200 crank angle degrees.

objective. This means that the information contained in the pressure is not entirely available to the model identification procedure. A PCA approach is proposed next as a way to compress the entire information available in the pressure profile in as few parameters as possible.

Consider a set of r operating points (i.e., couples of speed and injected fuel amount) scattered over the engine operating region as exemplified in Fig. 2 (where $r = 48$). The pressure profile varies considerably from one point to another, due to changes in airpath and combustion variables generating the pressure curve (see again Fig. 1). In Fig. 3, the large spread of the indicated pressure along the engine map is illustrated.

The first step is to find a way to describe all possible pressure profiles with a limited number of features. Intuitively, it does not seem necessary to use all 360 points, as the curves have much in common. These common "features" can be extracted using machine learning, pattern recognition, and data-mining fields. In this brief, PCA is suggested and implemented as it offers a good tradeoff between accuracy, simplicity, and computational efficiency (see [11]).

The PCA, also known as Karhunen–Loéve transform [11], is a method widely used in dimensionality reduction and feature extraction. PCA projects the data onto a lower dimensional subspace, such that the mean squared distance between the data points and their projection is minimized.

Consider the pressure matrix P built using the r pressure profiles (the size of P is then $r \times 360$). P can be rewritten as

$$P = U \Sigma V = \sum_{i=1}^{r} \sigma_i u_i v_i^T$$

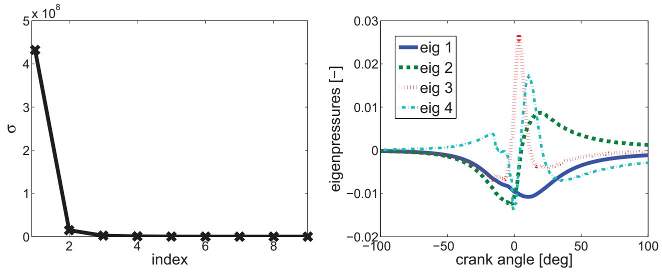

(a) (b)

Fig. 4. Singular values σ_i, $i = 1, 2, \ldots$, for principal component decomposition of (a) in-cylinder pressure and (b) eigenpressures related to the first four terms.

where u_i and v_i are suitable orthogonal vectors, U and V are matrices composed by joining u_i and v_i, respectively, and Σ is a diagonal matrix composed by the σ_i terms, $i = 1, \ldots, r$. The singular values σ_is give an idea of the relevance of each component in P and the singular value decomposition approach guarantees that the vectors are sorted according to their relevance. It is then possible to reconstruct P with $m < r$ terms, with accuracy bounded by

$$\varepsilon_j = \sum_{i=m+1}^{r} \sigma_i^2.$$

The first m features f_i, $i = 1, \ldots, m$, of a given profile p^* can be obtained by simply projecting such a profile over the first m eigenvectors (or "eigenpressures") $\bar{p}_i$, $i = 1, \ldots, m$

$$f_i = < p^*, \bar{p}_i >, \quad i = 1, \ldots, m \tag{1}$$

where $< \cdot, \cdot >$ denotes the inner product.

Fig. 4 represents the first nine singular values for the defined P and it shows that the most important elements in determining the pressure profile are the first four terms. This fact is due to geometrical reasons, as can be evaluated by the corresponding first four eigenpressures, shown in Fig. 4. The first component clearly determines the main "bell" shape of every profile among all 48 operating points. The second component weighs the distinction between the pilot injection and the main injection. The third feature is useful to reconstruct the pressure when the main peak is very pronounced. In addition, both the third and the fourth components help in following the nonlinear behavior of the pilot injection peak.

By employing only the first four eigenpressures, the reconstruction performance from feature extraction is satisfactory, as illustrated in Fig. 5 for three sample operating points out of the grid of Fig. 2.

Once the eigenpressures are fixed, the pressure information contained in 360 points can be "compressed" in only four numerical features, without substantial loss of information. The main features are then well-suited to represent the pressure as input of the NO_x estimation model.

III. Nonlinear Modeling

To estimate NO_x emission from in-cylinder pressure information, a model of the relationship between the pressure features and NO_x is needed. In the present case, the engine speed will also be included, to provide the link between crank angle domain and time domain. This choice will also be experimentally motivated in Section IV. In this section, a static polynomial structure for the model containing both pressure and speed will be taken into account and a system identification method will be studied for this special model class.

A. Polynomial Modeling and Convex Optimization

The main advantage of deriving NO_x information from in-cylinder pressure is that combustion and airpath dynamics are the cause of the pressure profile. This implies that the relationship between pressure and NO_x can be assumed to be static and the main problems related to nonlinear dynamic identification (see [10]) can be avoided. In the statistical and control literature, there are many different ways to identify a nonlinear static model for a multi-input, single-output system, see [12] for neural networks, [13] for support vector machines, and [14] for many other different statistical black box methods. Most of them are based on nonconvex optimization techniques and require considerable computational effort. The assumption of static system structure enables the use of simpler and more efficient methods without jeopardizing accuracy. More specifically, this brief will focus on linearly parameterized models with polynomial nonlinearities, in order to resort to convex optimization techniques. This choice also enables possible extensions to control-oriented adaptive on-line modeling.

Consider the unknown (noisy) static relationship between NO_x emissions $y(t)$ and the input vector $u(t)$ containing the selected inputs (i.e., $u(t)$ is such that u_i, $i = 1, \ldots, 4$ represent the four pressure features and u_5 is the engine speed). The I/O transformation reads $y(t) = f(u(t)) + v(t)$, where $v(t)$ is a zero mean white process modeling the measurement noise. Consider now the linear-in-parameters estimator $\hat{y}(t)$ for NO_x emission $\hat{y}(t) = \varphi(t)^T\theta$, where $\varphi(t)$ contains measured and/or calculated values based on inputs and θ is the parameter vector. More specifically, since a polynomial structure is considered, $\varphi(t)$ will contain all polynomial regressors up to an order l at the sampling instance t

$$\varphi(t) = [1,\ u_1(t),\ \ldots, u_5(t),\ \ldots,\ u_1(t)u_2(t),\ \ldots,\ u_5^l(t)]^T.$$

Notice that $\varphi(t)$ contains not only powered versions of u_i, but also cross-products of all the regressors, as this choice allows for modeling the nonlinear coupling among inputs, too.

The least squares method yields the optimal parameter estimate $\hat{\theta}$

$$\hat{\theta}_N = \left[\sum_{t=1}^{N} \varphi(t)\varphi^T(t)\right]^{-1} \sum_{t=1}^{N} \varphi(t)y(t). \tag{2}$$

Although the proposed model is numerically efficient (due to linear parameterization) where N measurements of $\varphi(t)$ and $y(t)$ are available, it is worth noting that the complexity grows factorially with the regressor dimension n_θ. As a matter of fact, it holds that (see [15] for further details)

$$n_\theta = \sum_{k=0}^{l} \binom{i+4}{i} = \sum_{k=0}^{l} \frac{(4+i)!}{i!4!}.$$

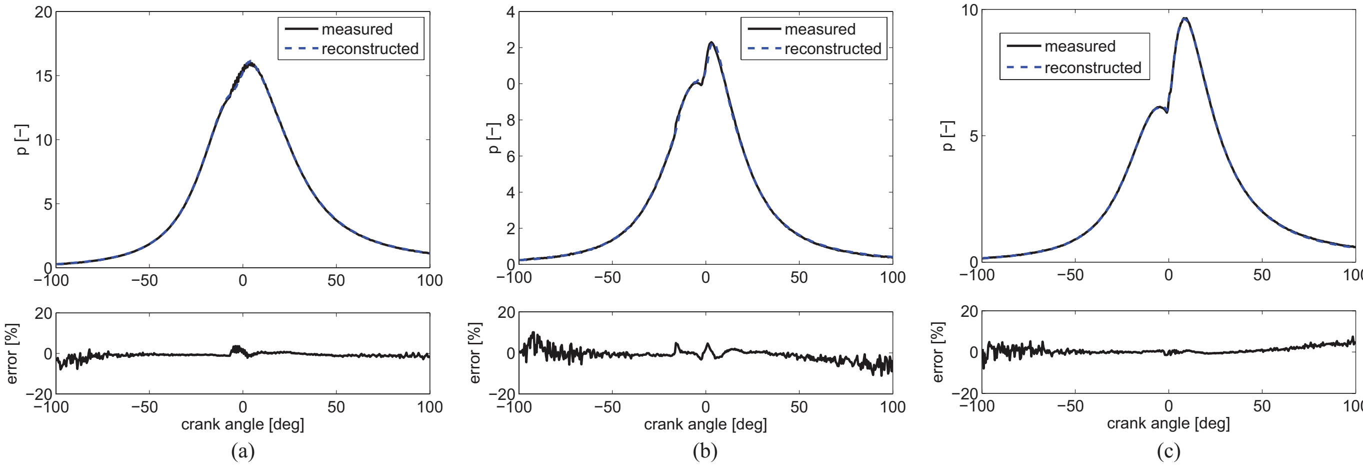

Fig. 5. Pressure profile reconstruction and error plots for three different operating point samples.

It is therefore important to accurately choose the order l of the regressors. This will be done in the next section, where also a regularization method will be introduced to make the problem numerically well-conditioned.

B. Subset Selection and Regularization

When the regressor dimension is high, numerical issues (see [16]) related to a badly conditioned regressor matrix may arise. L_1 or L_2 regularization alleviate this problem by selecting a subset of regressors to use in the Gauss formula (2). On the one hand, among L_1 methods, the LASSO approach introduced in [17] and [18] gives very good results in terms of model error. On the other hand, L_2 methods (and especially the iterative scaled ridge regression (ISRR) approach, proposed in [19]) are less accurate but computationally faster than the LASSO approach. Therefore, L_2 solutions are preferred in this case, as simple and fast-to-identify models are the object of this brief (see again the discussion in Section I) and acceptable performance can still be guaranteed.

The ISRR algorithm defines a "regularized" version of (2), namely $\hat{\theta}^{(2)}$, parameterized through k

$$\hat{\theta}^{(k)} = \left(\sum_{t=1}^{N} \varphi(t)\varphi^T(t) + \lambda_k D_k^{-2}\right) \sum_{t=1}^{N} \varphi(t) y(t)$$
$$D_k = \operatorname{diag}\left(\frac{\hat{\theta}_i^{(k-1)}}{\zeta}\right)$$

where ζ is an estimate of the noise standard deviation and λ_k are n_k "regularization parameters" such that $\lambda_0 = 0 < \lambda_1 < \cdots \lambda_{n_k} = 1$. Like in any regularization procedure, the penalty term $\lambda_k D_k^{-2}$ modifies the information matrix in order to put in evidence the relevant regressors.

In [19], it has been shown that the optimal k and the subsequent value of λ can be selected by minimizing a suitable evaluation criterion. Here, the generalized cross validation (GCV) criterion is minimized with respect to λ to find the optimal model parameters and disregard the unimportant regressors. The formal definition of GCV is as follows:

$$\mathrm{GCV}(\lambda) = \frac{1}{N} \frac{\|(I - A(\lambda))\, Y\|^2}{\left[\frac{1}{N} \operatorname{trace}(I - A(\lambda))\right]}$$

where $Y = [y(1)\ y(2)\ \cdots\ y(N)]^T$

$$A(\lambda) = \sum_{t=1}^{N} \varphi^T(t) \left(\sum_{t=1}^{N} \varphi(t)\varphi^T(t) + \lambda I_{n_\theta}\right) \varphi(t)$$

and I_{n_θ} is the identity matrix of dimension n_θ. Properties of such an evaluation criterion are described in detail in [20]. The method has many advantages, e.g., its effectiveness holds also in case of undermodeling and it is purely data-driven.

A very interesting feature of the proposed method is its low computational burden. Specifically, once n_θ and the number of features m is fixed, the list of the operations required for each sampling time to the ECU is the following:

1) m scalar products between the (available) eigenpressures and the measurement of the indicated pressure, to compute the features. This is equivalent to $360 \times m$ multiplications (m for each crank angle position, provided the resolution is 1 degree) plus $359 \times m$ sums;
2) n_θ products between the coefficients of the model and the selected regressors;
3) $n_\theta - 1$ sums to find the value of the NO_x emissions.

Therefore, the number of operations is $O(n_\theta, m)$.

IV. Experimental Results

A. Testbench Setup

All the analyses were done on an AVL dynamical engine test-bed at the Johannes Kepler University Linz with a temperature conditioning of the test-cell and fresh air delivery for the engine being controlled in temperature and humidity. The fuel temperature is controlled, too. The test candidate is a 7-liter four-cylinder HD off-road Diesel engine with dual stage turbocharging, high pressure direct fuel injection, and a nominal power of 175 kW (see Table I). All four cylinders are equipped with Kistler indicated pressure measurement sensors

TABLE I
ENGINE DATA

Cylinders	4
Bore	122 mm
Stroke	150 mm
Compression ratio	17.4
Air system	2 stage turbocharger and high pressure EGR
Max. torque	1250 Nm
Nominal power	175 kW
Nominal speed	2000 rpm

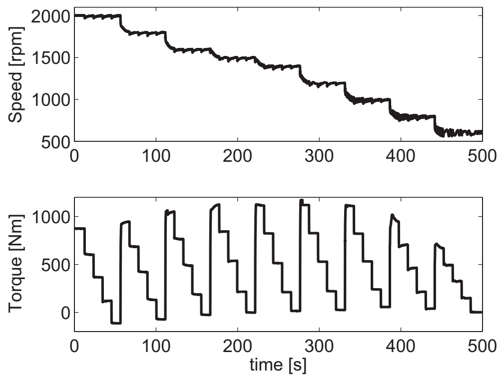

Fig. 6. Speed and torque trajectories for the grid measurement test for identification.

and the data acquisition is done with a dSpace rapid protoyping system and a Smetec indicated pressure measurement system. NO_x emissions are measured with two measurement devices—a Horiba Mexa7100 for the grid measurements and the fast Cambustion $f NO_x 400$ ($t_{10,90} < 10$ ms) for the transient analyses.

B. Order Selection and Identification

Consider a measurement grid dataset spanning the whole engine operating range. Fig. 6 represents a possible experiment to collect such data. Since this kind of experiment visits many (i.e., 45 in this case) steady-state points, the eigenpressures can be easily obtained as illustrated in Section II. The set of main features is then derived by projecting the pressure profiles onto the subspace defined by the eigenpressures (see Fig. 7). Moreover, since for each emission sensor more than one cycle is available depending on the engine speed, the mean pressure profile is computed over the interval for each NO_x sample.

The value of λ for optimal regularization has been chosen over $n_{\text{iter}} = 50$ iterations as the minimizer of the GCV criterion, as explained in Section III-B. Different values of model order l have been tested on the validation cycle that will be presented in the next section. Table II suggests that the quadratic model ($l = 2$) with cross products is the best choice, as it provides a regressor with small input dimension and with low estimation error. The case of $l = 1$ is not sufficient to match all the important dynamics, whereas $l = 3$ causes overfitting. Table II also quantifies the importance of cross-terms in the regressor matrix for $l = 2$ (the normalized mean error decreases).

By performing the static model identification as described in Section III, the optimal θ provides an estimator whose

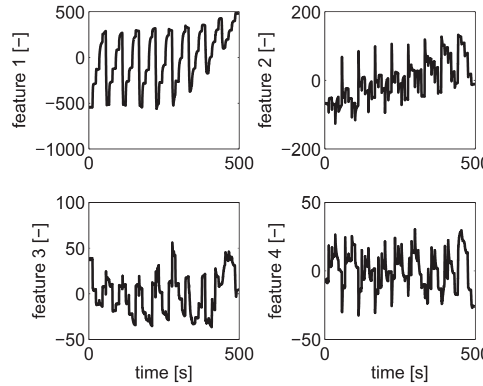

Fig. 7. Feature trajectories for the grid measurement test for identification.

TABLE II
MEAN ESTIMATION ERROR (NORMALIZED WITH RESPECT TO THE MAXIMUM NO_x) FOR DIFFERENT MODEL ORDERS WITH (W) AND WITHOUT (W/O) CROSS-PRODUCTS

Polynomial Order	Normalized Mean Estimation Error [%]
l=1 w/o cross-products	0.87671
l=1 w cross-products	1.8280
l=2 w/o cross-products	3.6030
l=2 w cross-products	0.4779
l=3 w/o cross-products	2.6685
l=3 w cross-products	2.7213

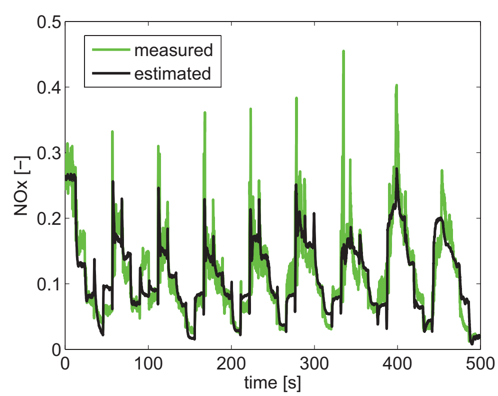

Fig. 8. Estimation performance on the identification dataset.

performance on the identification dataset is illustrated in Fig. 8. Estimation results are quite satisfactory (the normalized mean estimation error is 0.1757%); however, this is not sufficient to assess the quality of the estimator; a validation test on a different dataset is needed. In the rest of the section, two different validation tests will evaluate the behavior of the estimator.

C. Wheel-Loader Cycle

Fig. 9 depicts the speed and torque trajectories of a HD wheel-loader application. Once the eigenpressures and the model parameters are derived from the first experiment, the estimator can be directly tested on a different dataset. It should be stressed here that the eigenpressures have to be generated only in the first "tuning" experiment and do not need to be

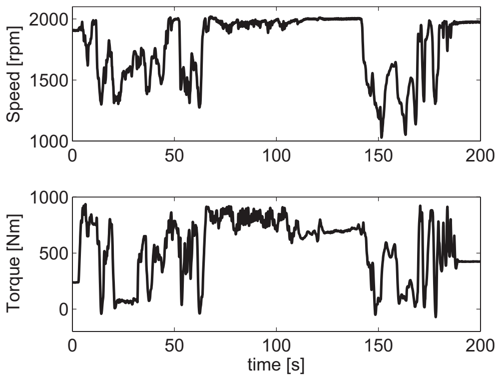

Fig. 9. Speed and torque trajectories of the wheel-loader application.

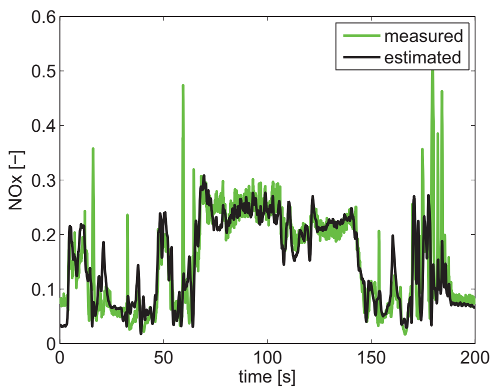

Fig. 10. Estimation performance on the wheel-loader cycle.

calculated again when the cycle changes. The final algorithm is suitable for both on-line and off-line NO_x estimation. To summarize, the procedure is very fast and only two steps are required for its implementation:

1) each step (sampling time), the mean pressure profile is projected over the cycle on the same eigenspace obtained from Experiment 1, in order to get the new features;
2) a new NO_x estimation is computed by using the features at the previous point and the model parameters from Experiment 1.

The estimation performance is shown in Fig. 10. The behavior is as expected: the static model allows the NO_x trajectory to be captured in an accurate way whenever the static assumption is verified (in this case, the mean estimation error, normalized with respect to the maximum NO_x, is 0.4779%). The proposed method is, however, not capable of precisely predicting transient peaks, as these phenomena are not included in the identification experiment. This does not limit the applicability of the proposed method to NO_x aftertreatment and closed-loop combustion control.

In particular for the aftertreatment control, the low-frequency behavior is very important, to such an extent that, in engine control practice, the viability of the emission estimation method is assessed, among other indicators, by the difference between time-integral of the measured and estimated NO_x values. Fig. 11 evaluates the present estimator from this point of view. Notice that only about 0.7103% error is piled up after 200 s (i.e., 2000 samples).

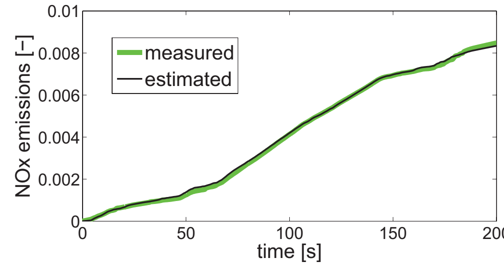

Fig. 11. Integral value of NO_x measurement and estimation over time.

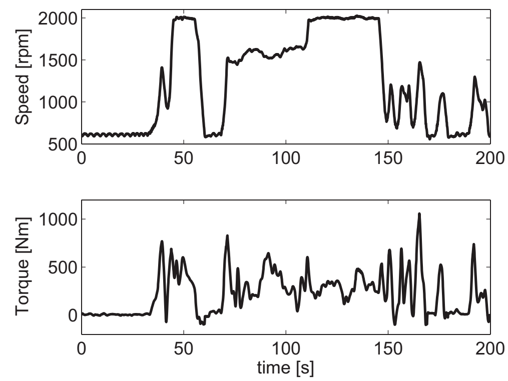

Fig. 12. Speed and torque trajectories of the standard NRTC.

D. Nonroad Transient Cycle (NRTC)

This section aims at highlighting that, even if based on a static model, the proposed estimator provides good performance also for transient test. This is due to the use of in-cylinder pressure instead of airpath and combustion parameters, typically characterized by slower dynamics with respect to emission generation. The test proposed herein is the NRTC depicted in Fig. 12. Like in the wheel-loader cycle case, the main features can be derived with the two simple steps described at the beginning of the last section.

It should be here recalled that the eigenpressures are once again the same previously identified using the grid test. The final estimation performance is then shown in Fig. 13.

Even if some dynamics are still existing and evident from the figure, the accuracy of estimation is acceptable (in this case, the normalized mean estimation error is 2.9877%).

E. Sensitivity Analysis

In the previous analysis, the initial choice of four features has been employed. It is interesting to investigate the sensitivity of the method to the number of features employed. More specifically, Fig. 14 shows that the above choice of four features represents a good tradeoff between a low-informative choice (two features) and a high-variance selection (ten features) on the wheel-loader application. This phenomenon can be easily explained by thinking that a low number of features does not contain all the information to reconstruct the profile, and that the variance of the NO_x estimation error $\varepsilon(t) = \hat{y}(t) - y(t)$ is linearly dependent on the variance of the parameter vector, see [21] (therefore, the bigger the vector dimension is, the larger the estimation variance is). In other words, the latter

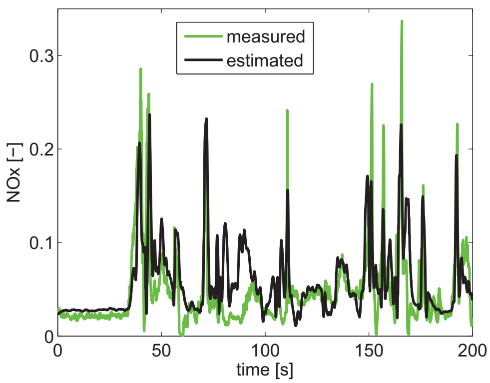

(a)

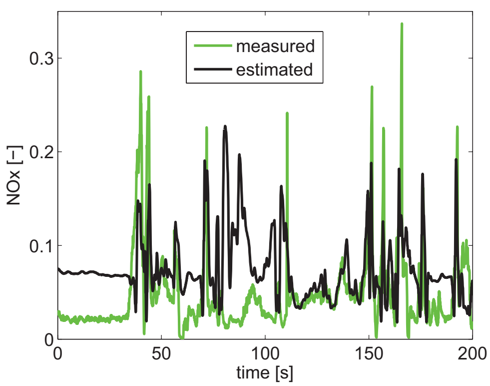

(b)

Fig. 13. Estimation performance on the NRTC (a) with and (b) without speed information.

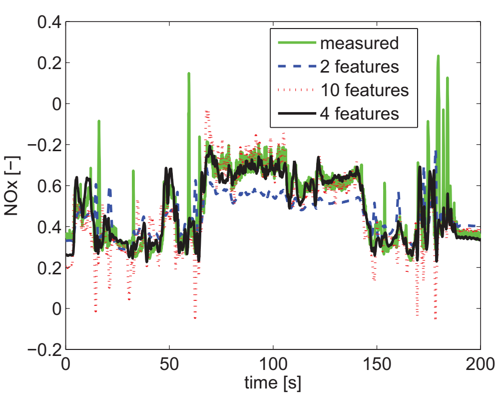

Fig. 14. Sensitivity to the number of pressure features.

phenomenon is due to overfitting of identification dataset, as confirmed in Table III, where the normalized mean estimation error is shown for both identification and validation datasets.

Notice that in case of NO_x estimation with ten features, the NO_x estimator becomes negative and additional information (i.e., a saturation term) would need to be added.

Another interesting aspect to analyze is the effect of additional information, i.e., adding other combustion related regressors to the identification. Fig. 15 illustrates the integral value of the error for different input sets: pressure and speed only, pressure and speed with angle of main injection, pressure and speed with EGR valve position, pressure and speed with rail pressure. It is clear that the traditional combustion and

TABLE III

SENSITIVITY OF THE MEAN ESTIMATION ERROR MSE (NORMALIZED WITH RESPECT TO THE MAXIMUM NO_x) TO THE NUMBER OF FEATURES

No. of Features	Dataset	Normalized MSE [%]
2	**grid test**	0.0312
2	**standard off-road cycle**	4.1010
4	**grid test**	0.0329
4	**standard off-road cycle**	0.4779
10	**grid test**	0.0176
10	**standard off-road cycle**	0.6654

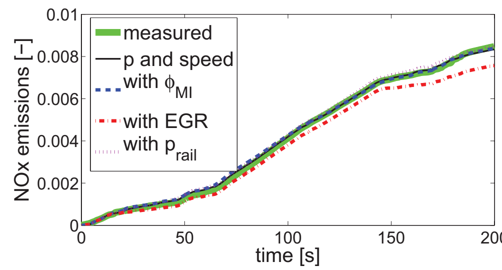

Fig. 15. Integral value of NO_x measurement and estimation over time for different input sets: measured emissions (thick solid line), estimation with pressure and speed (thin solid line), with pressure, speed, and angle of main injection (dashed line), with pressure, speed, and EGR valve position (dash-dotted line), with pressure, speed, and rail pressure (dotted line).

airpath variables are either redundant or misleading with respect to the in-cylinder pressure (for what concerns NO_x estimation) and that therefore pressure and engine speed are sufficient to describe NO_x generation.

It should be mentioned that a lot of engine operating conditions are visited in the test in Fig. 15 and the range of the combustion and airpath variables is large.

Finally, the NRTC cycle will be used to highlight the importance of engine speed in building the estimator. In Fig. 13(b), the estimate without engine speed confirms that the crank angle domain pressure is not informative enough for building an accurate static model for NO_x estimation purpose.

V. CONCLUSION

In this brief, an empirical approach was presented for NO_x estimation based on PCA and L_2 techniques applied on indicated pressure measurements. An interesting aspect of the approach is that it provides a "crank angle-based mean value model" of the NO_x emissions, i.e., mean values were extracted from the crank angle-based pressure measurement and then used as input for a mean value model of the NO_x emissions. In order to provide satisfactory results for the whole engine operating range, besides the indicated pressure, the engine speed information was used as additional input to link crank angle domain and time domain. As the PCA showed, four features are sufficient to capture the pressure traces with high accuracy. Notice that the required number of features might increase in case a wider operating range was considered, e.g., combustion mode changes. Moreover, a simple static polynomial model can provide a valuable estimation of the

NO_x values, during steady state and during transient validations. All in all, the presented approach provided not only a satisfactory NO_x estimator, but also a model which could be used as a basis for closed-loop combustion control as well as for NO_x after treatment devices.

Future work will focus on the improvement of the transient performance and on the design of closed-loop control systems based on the presented model.

REFERENCES

[1] I. Lilly, *Diesel Engine Reference Book*. London, U.K.: Butterworth, 1984.

[2] A. Elia, C. Di Franco, A. Afzal, N. Cioffi, and L. Torsi, *Advanced NO_x Sensors for Mechatronic Applications*. Triangle Park, NC, USA: InTech, 2011.

[3] T. Husberg, I. Denbratt, J. Engstrom, and M. Ringvik, "Heavy-duty diesel combustion with ultra-low NO_x and SOOT emissions: A comparison between experimental data and CFD simulations," in *Proc. SAE World Congr.*, 2005, DOI:10.4271/2005-01-0380.

[4] A. Schilling, A. Amstutz, C. Onder, and L. Guzzella, "Real-time model for the prediction of the NO_x emissions in DI diesel engines," in *Proc. IEEE Int. Conf. Control Appl.*, Oct. 2006, pp. 2042–2047.

[5] J. Bayer and D. Foster, "Zero-dimensional soot modeling," *SAE Trans.*, vol. 112, no. 3, pp. 1446–1458, Mar. 2003.

[6] K. S. Oppenauer and L. del Re, "Hybrid 2-zone diesel combustion model for NO formation," *SAE Int. J. Eng.*, vol. 2, no. 2, pp. 584–596, Mar. 2010.

[7] M. Hirsch and L. Del Re, "Adapted D-optimal experimental design for transient emission models of diesel engines," in *Proc. SAE Tech. Paper*, 2009, pp. 0601–0621.

[8] M. Hirsch, D. Alberer, and L. del Re, "Grey-box control oriented emissions models," in *Proc. IFAC World Congr.*, Jul. 2008, pp. 8514–8519.

[9] M. Traver, R. Atkinson, and C. Atkinson, "Neural network-based diesel engine emissions prediction using in-cylinder combustion pressure," *SAE Trans.*, vol. 108, no. 4, pp. 1166–1180, May 1999.

[10] A. Juditsky, H. Hjalmarsson, A. Benveniste, B. Delyon, L. Ljung, J. Sjoberg, and Q. Zhang, "Nonlinear black-box models in system identification: Mathematical foundations," *Automatica*, vol. 31, no. 12, pp. 1725–1750, Mar. 1995.

[11] I. Jolliffe, *Principal Component Analysis*. New York, USA: Wiley, 2005.

[12] W. Miller, R. Sutton, and P. Werbos, *Neural Networks for Control*. Cambridge, MA, USA: MIT Press, 1995.

[13] L. Wang, *Support Vector Machines: Theory and Applications*. New York, USA: Springer-Verlag, 2005.

[14] J. Suykens and J. Vandewalle, *Nonlinear Modeling: Advanced Black-Box Techniques*. New York, USA: Springer-Verlag, 1998.

[15] M. Hirsch, "Identification of a virtual sensor model for diesel engine emissions by means of optimal input design," Ph.D. dissertation, Inst. Design Control Mech. Syst., Johannes Kepler Univ., Linz, Austria, 2011.

[16] I. Guyon and A. Elisseeff, "An introduction to variable and feature selection," *J. Mach. Learn. Res.*, vol. 3, no. 3, pp. 1157–1182, Mar. 2003.

[17] R. Tibshirani, "Regression shrinkage and selection via the lasso," *J. Royal Stat. Soc. Ser. B*, vol. 58, no. 1, pp. 267–288, Jan. 1996.

[18] N. Meinshausen and P. Buhlmann, "High-dimensional graphs and variable selection with the lasso," *Ann. Stat.*, vol. 34, no. 3, pp. 1436–1462, 2006.

[19] G. Bortolin and P. Gutman, "A new algorithm for variable selection," in *Proc. 45th IEEE Conf. Decision Control*, Dec. 2006, pp. 1309–1314.

[20] G. Golub, M. Heath, and G. Wahba, "Generalized cross-validation as a method for choosing a good ridge parameter," *Technometrics*, vol. 21, no. 2, pp. 215–223, 1979.

[21] L. Ljung, *System Identification: Theory for the User*. Englewood Cliffs, NJ, USA: Prentice-Hall, 1999.